Improving the Geometry of Manholes Designed for Separate Sewer Systems

Alaa Abbas [1], Felicite Ruddock[2], Rafid Alkhaddar[3], Glynn Rothwell[4] and Robert Andoh[5]

[1] Postgraduate Research Student, Liverpool John Moores University, Department of Civil Engineering, Henry Cotton Building, 15-21 Webster Street, Liverpool, L3 2ET, UK, A.H.Abbas@2015.ljmu.ac.uk
[2] Programme Leader, Department of Civil Engineering, Liverpool John Moores University, Peter Jost Center, Byrom Street, Liverpool L3 3AF, UK, F.M.Ruddock@ljmu.ac.uk.
[3] Professor of Water and Environmental Engineering and Head of the Department of Civil Engineering, Liverpool John Moores University, The Peter Jost Center, Byrom Street, Liverpool, L3 3AF, UK, R.M.Alkhaddar@ljmu.ac.uk
[4] Department of Maritime and Mechanical Engineering, Liverpool John Moores University, Byrom Street, Liverpool, L3 3AF, UK,G.Rothwell@ljmu.ac.uk
[5] Professor Robert Andoh, CEO and President of AWD Consult Inc. 32 Vista Drive, South Portland, ME 04106, USA, bandoh@awdconsult.com

Abstract

The design of manholes dates back more than 100 years. However, there have been developments such as the use of new materials for the manufacture of manholes, and advances in inspection and maintenance technologies, allowing improvements to the shape of manholes. This paper presents an innovative design for manholes, created to overcome the challenges associated with the installation of separate sewer systems in narrow streets, common to both UK and EU cities. The traditional separate sewer system has two separate manholes. The proposed manhole combines these two manholes into one structure, with two separate chambers, to allow storm flow and foul flow to pass through the same manhole without mixing. The structural performance of the new design has been tested using mathematical modelling validated by experimental tests. The results are compared with the structural performance of traditional manholes. The new design shows an improved resistance to high live loads.

Keywords: Innovative design, manhole, mathematical model, separate sewer system, structural performance.

1. Introduction

The manhole is one of the main elements of a sewer network, used to gain access to the sewer for inspection and maintenance. The construction of manholes has improved, over time, with reference to the materials used. Originally built of brick, significant improvements were made by using concrete and precast materials. However, corrosion to concrete caused by H_2S means that the inner surface of manholes need to be coated, or newly developed materials such as fiberglass and polyethylene used instead (Ahn et al. 2009; Hughes 2009; Petroff 1994). A manhole needs to provide sufficient working space and safe entry and egress for personnel to the sewer system network (BSEN476 2011). Recently, because of rapid developments in sewer inspection and maintenance equipment technology, many water authorities have started using inspection manholes, instead of the traditional manhole, which has the same design of a manhole but with smaller dimensions, this manhole suitable for equipment entry rather than personnel access (BSEN752:2008 2013). The maximum space between two manholes and location of the manhole should be adequate to allow easy use of this equipment. This means that design criteria require manholes sited at every change of alignment, or gradient, and wherever there is a change in the size of sewer pipes. They also need to be spaced at reasonable intervals for inspection and maintenance, somewhere between 50 and 100 meters (BSEN752:2008 2013). Manholes are either rectangular or circular, but from a review of the literature, it is clear that there is a paucity of research on manhole shape or structural performance (Bettez et al. (2001); Saricimen et al. (2003)), specifically regarding combined manholes. A rectangular combined manhole, one manhole structure with two chambers, one for wastewater the other for rainwater, was patented by Würmseher (2014). Willi (1998) patented a design which was the same size as traditional manholes but can be either rectangular or circular with two stage chambers arranged vertically, storm chamber over sanitary. Work examining the structural performance of traditional manholes was carried out by Sabouni and El Naggar (2011a). They used three manholes, two of diameter 1200 mm (one reinforced, the other not), the third of diameter 1500 mm, both built from precast concrete. They used a large-scale (4.5 m x 4.5 m x 7.62 m) geotechnical cell for testing and followed the Canadian Highway Bridge Design Code as a guide for the application of live loads. They found that the range of

displacement of the manholes ranged between 1.3 mm and 5.6 mm for all loading tests. They concluded that the frictional resistance along the manhole structure, mitigated the effect of truck loading. All their manholes withstood the truck loads, even the non-reinforced one. Sabouni and El Naggar (2011b) used these results to validate a 3-dimensional Finite Element model (FE) for circular, precast and concrete manholes. The FE model was used to test a different combination of concrete manholes in native soil conditions, including soil compaction, groundwater level, trench dimensions and method of installation. They found that soil water content (groundwater level) creates more stress effects on manhole bases than any other factor. Al-Saleem and Langdon (2016) presented the results of structural tests of a manhole under a single live load, this was part of work to develop and upgrade standardised design guidelines for precast concrete manholes in New Zealand (CPAA 2016). They concluded that the service life of a manhole is typically 100 years and that the designer needs to be aware that the standard design is for normal application but that the manhole can be modified to meet any special site requirements or project applications. IKT (2012) who estimated the total number of manholes in Germany at ten million, conducted a full-scale comparison laboratory experiment study, using cementitious and polymeric coatings to line manholes to improve their structure, and to treat those which were deteriorating. A substantial study was carried out by Najafi and Sever (2015b), who estimated the number of manholes in the USA to be approximately 20 million. Their study tested the structural capabilities of the manhole when lined with specific materials using structure strength tests, mathematical modelling and evaluated case histories. The procedure involved using a small-scale model to validate an FE model, the results of which were used to upgrade the FE model to full scale. The results from both Germany and the USA, revealed that manhole structural performance was not affected by the type of lining or deterioration of said lining. Bandler (2007) conducted a study to test two types of manhole materials; unreinforced concrete and masonry. Manholes were exposed to axisymmetric pressure to simulate horizontal effective loads, the effect of the coating material assessed in order to improve the structural performance of the manhole. Brown and Brown (2000) studied the structural performance of manholes and the combination of vicinity asphalt surfacing under wheel loadings, finding that surface displacement is a result of subgrade deformation rather than manhole deformation.

This paper presents a new design for manholes, gathering the two separate sewer manholes (sanitary manhole and storm manhole) into one manhole structure with two separate chambers, one for sewage flow the other for stormwater flow. This new design provides the advantages of decreases in cost and a reduced footprint compared with traditional separate sewer systems, as it allows two pipes to be positioned in one trench and the construction of separate sewer systems in narrow streets. The structural performance (correlation between manhole shape and soil) of the new manhole when buried in soil, was tested in this research. Two prototypes were used; the new design and a traditional manhole. The experimental results were used to validate a numerical model which upgraded the model to real scale. The integrity of the structural performance of the new design has been tested and compared with the structural performance of traditional manholes under the same conditions.

2. Design Loads

The manhole structure can be exposed to two types of loads; permanent dead loads such as the weight of the manhole structure, road layers, soil backfill and manhole cover, and live loads such as traffic loads and hydrostatic flow load. The traffic load directly effects the manhole cover as it is normally on same level as the street surface. Table 1 shows the different categories of live loads (ASTM-C890 2006; BS 2010). The manhole wall needs to be thick enough to resist the compressive forces caused by vertical loads and/or horizontal loads such as lateral earth pressure or hydrostatic pressure (ACPA 2008) . The lateral load pressure can be calculated as:

$$p = w_s H K_s + 62.4H$$

where p = total earth and hydrostatic pressure (pounds per square foot); w_s = effective unit weight of backfill material (pounds per cubic feet); H = depth of manhole (feet) and K_s = the conjugate ratio for the soil.

ASTM-C890 (2006) uses a pyramid method to calculate the distribution of traffic loading through specific cover depths (H) such as pavement layers and filling soil above the structure of the manhole, Equation 1 is used to calculate this load. The tire footprint for dual wheels is simulated by a rectangular plate (L=50.8 cm x W=25.4cm), the pressure on the manhole structure being the pressure at the base of the pyramid. Figures 1 and 2 show the distribution of dead loads and live loads on the manholes. In this research, H is taken as zero to apply the maximum load that the top of the manhole can be exposed to.

$$P=F/(W+1.75H)\times(L+1.75H) \quad \ldots\ldots \text{ (Eq 1)}$$

Fig. 1. Pyramid method for the distribution of a live load "Reproduced, with permission from [ASTM C890-13] copyright ASTM International, 100 Barr Harbor Drive, West Conshohocken, PA 19428."

Fig. 2. cumulative vertical loads "Reproduced, with permission from [ASTM C890-13] copyright ASTM International, 100 Barr Harbor Drive, West Conshohocken, PA 19428."

3. Manhole models

The conventional, separate sewer system has two manholes; one for sewage, the other for stormwater. The geometrical design of these manholes was created more than 100 years ago, Figure 3 illustrating this design and its setup within a traditional separate sewer system (DEFRA 2011). Normally the dimensions of the conventional manhole are between 1 and 1.8 meters diameter at the intermediate network (between the lateral pipes and trunk pipelines), the exact size dependant on the diameter of the inlet-outlet pipe servicing that manhole. The depth of the manhole is dependent on the level of the outlet pipe and can be 1 meter at the beginning of the network, increasing to a depth of 7 meters before using a lift station to raise the hydraulic gradient again to 1 meter. Novel approaches, techniques and devices mean that the original design criteria established a century ago, is obsolete. The negative impact of the combined sewer system on the environment has necessitated new environmental regulations to encourage the use of separate sewer systems (Bizier 2007). Work is required to comply with new regulations for the protection of the environment, even in areas where the installation of traditional separate sewer systems is challenging (EPA 2007).

Fig. 3. Typical design of a sanitary manhole and storm manhole located in a separate sewer system

147 This research constitutes a new approach to manhole design by combining the two manholes in a
148 separate system, into a one-manhole structure still keeping both storm flow and sewage flow separate.
149 The new structure has two chambers; an external chamber for stormwater flow and an inner chamber
150 for sewage flow. Figure 4 details the design of the new manhole, Figure 5 detailing a cross section of
151 the new manhole in the street. The first chamber, the outer chamber, has a stormwater inlet and a
152 separate stormwater outlet. The second chamber comprises a sewage inlet and separate sewage outlet.
153 The two chambers are arranged coaxially, the storm pipe set above the sanitary pipe in one trench.
154 The dimensions of the outer chamber are between 2.5 to 3 meters diameter, the depth relative to the
155 level of the storm pipes (both inlet and outlet). The dimensions of the inner chamber range from 0.8 to
156 1.2 meters, the depth dependant on the level of the sanitary pipes (inlet and outlet).
157 The manhole itself can be concrete or plastic e.g. HDPE, PVC or GRP, the same material available for
158 traditional manhole manufacture. Because of this, there should be no difference in the lifetime service
159 of the new manhole in comparison to a traditional manhole. The hydraulic performance of the new
160 manhole however, has a different impact on the serviceability of the sewer system, this requiring more
161 research to establish the hydraulic integrity of the new design. A non-reinforced concrete manhole
162 was used to simulate a real scale model in this research.
163
164

Fig. 4. Innovative design of a manhole for separate sewer systems.

165
166

Fig. 5. Cross section of new manhole located in a separate sewer system.

167
168
169
170

4. Methodology

A two-stage approach was followed in this research. In the first stage, the finite element model for the case study was built with all the input criteria determined using lab tests to identify the properties of the materials. Prototypes and experimental work were used to identify the boundary conditions necessary to validate the results from the mathematical model (Brinkgreve 2013). The second stage used the mathematical model to ascertain the real scale dimensions of both manholes; the traditional manhole and new design manhole. The FEA used ABAQUS to test the manhole-soil correlation and identify degree of displacement under four loading categories; medium (HS15), heavy (HS20 and HS25) and one overload (double heavy traffic load) when two trucks pass over the manhole at the same time.

4.1 *Experimental Work*

Two prototypes, one of a traditional manhole with a diameter of 10 cm and depth of 30 cm, the other of the new design with the same dimensions for the inner chamber but with a diameter of 25 cm and depth of 25 cm for the external chamber, were constructed. The manholes were buried in soil in a trench of dimensions 2.5 x 0.5 x1 meters. The trench was located in a hydraulic rig which was used to apply live loads. The cell load and Linear Variable Differential Transducers (LVDTs), were used to monitor applied loads and displacement of the manhole structure, the data recorded by an MC3 recorder. The results were used to validate the FE model, this validation allowing an upgrade to a real scale FE model. Figure 6 illustrates the setup of the trench in the rig, the buried manholes, the location of the load cell and the three (LVDTs) for the new manhole. Figure 7 shows the same set up for the traditional manhole. An important input parameter for the FE model concerns the properties of the materials used. Because this research focuses on the performance of the geometry of the manhole buried in soil and not the stress of the manhole structure, the soil properties have been identified through a series of geotechnical laboratory tests. These identified the degree of elastoplastic behaviour of the soil and the contact relationship between the external surface of the manhole and surrounding soil. A natural top-soil was used, normally available from the first layer of the ground

surface around the UK, as this is the zone where manholes are buried. As steel was used to build the prototype manholes, the friction factor between the steel surface and the soil was also determined.

a

b

Fig. 6. Setup of the trench in the rig and location of measurement instruments on the new manhole surface at three points on the edge.

a

b

Fig. 7. Setup of the trench in the rig and location of measurement instruments on the traditional manhole surface at three points on the edge.

4.2 *Mathematical model*

A wide range of tools are available to carry out finite element analyses (FEA), including commercial packages such as ABAQUS (used in this research), designed for use with complicated geotechnical issues (Torben Pichler 2012). The development of mathematical tools and improvements to the library of material applicable for FEA, allows geotechnical engineers to select which tools to use to successfully solve geotechnical structural problems and simulate structural behaviours when manholes are embedded in soil. That said, engineers still need to have both a geotechnical background and a good understanding of the principles of FEA to avoid misjudgements. Soil is a complex media because the texture of soil includes solid particles and voids, which can be full of air or water, making predicting and simulating soil behaviour a considerable challenge (Mar 2002). Two FE models have been created for the prototype simulation in the current research; one to simulate the new manhole, the other a traditional manhole. The same experimental conditions, dimensions, boundary conditions and materials were used. Restrictions at the base prevented movement but allowed displacement in the y-axis for the external model's faces and used the symmetry around the x-axis and z-axis for the internal faces to simulate the full model behaviour. The symmetry of the model around the x-axis and z-axis allows the use of a quarter model using the specific tools in Abaqus. The creation of a

symmetrical model and use of only one quarter of the model decreases the run time while giving the same results as a full 3D model . Surface to surface contact interaction was fixed with a friction factor 0.45 between the soil and steel, this determined from the experimental test. Figure 8 shows the mesh for the symmetrical quarter of the new manhole model which has 45370 nodes, 35350 elements, 35269 linear hexahedral elements of type C3D8R and 81 linear wedge elements of type C3D6. Figure 9 shows the mesh for the symmetrical quarter of the model of the traditional manhole which has 40532 nodes, 34928 elements, 34856 linear hexahedral elements of type C3D8R and 72 linear wedge elements of type C3D6.

Fig. 8. The symmetrical quarter of the new manhole FE mesh model representing the full 3D manhole.

Fig. 9. The symmetrical quarter of the traditional manhole FE mesh model representing the full 3D manhole.

5. Results and discussion

5.1 *Prototype experimental results*

Loads have been applied to verify the capacity of the new manhole compared to the traditional manhole, and to calculate the manhole shape – soil correlation. Four categories of loads were simulated; medium traffic HS15, heavy traffic HS20 and HS25 and overload (double heavy traffic). Figure 10 details the response of the new manhole under static applied loads, HS15, HS20, HS25, a double HS25 and a dynamic double HS25, applied load at the end of the test, to establish the maximum resistance. The displacement experienced by the new manhole was within acceptable limits, the standard requirement being 13 mm (Sabouni and El Naggar 2011a), when under HS15, HS20 and HS25 loadings. Displacement was 3.3 mm at HS15, 6.2 mm at HS20 and 9.2 mm at HS25. When the applied load was increased to over load (twice the heavy load HS25), the new manhole continued to be stable but the displacement was 22 mm, which is above acceptable limits. Soil density and the degree of compaction of the filling soil, play a significant role in the stability of buried

manholes under live loads (Abolmaali and Kararam 2010). Therefore, the same set of tests were applied to the traditional manhole, the results presented in Figure 10. Displacements were 2.9 mm for a load of HS15, 7 mm for HS20, 14.3 mm for HS25, the manhole sinking into the soil when HS25 was doubled. Steel was used to build the manhole prototype because of difficulties fabricating small prototypes of concrete. The friction factor between the steel and soil is less than the friction factor between concrete and soil meaning that the degree of displacement will be lower when concrete is used because the friction factor will be higher.

The comparisons between the displacement of the new manhole with the traditional manhole in Figure 10, show that under a medium load (HS15), the traditional manhole has less displacement compared to the new manhole. This is because the new manhole is heavier than the traditional one, this adding a significant dead load. However, the effect of manhole weight is smaller when the traffic load is increased. Against the application of heavy loads, the geometry of the manhole plays an important role, improving the resistance of the manhole.

Fig. 10. Comparison between the new and traditional manholes under the same conditions and live loads.

5.2 *The results from the mathematical model.*

The same series of loads (HS15, HS20 and HS25) and the exact boundary conditions as for the physical model, were applied on manholes using a finite element model. Selecting the proper constitutive model (stress–strain relationship) to simulate soil behaviour is an important aspect to consider when using FE for soil models (Lees 2012). In this research, two constitutive models (Mohr-Coulomb and Drucker-Prager) have been tested to identify the most appropriate model (Abbas et al. 2017). The properties of the soil were defined by conducting three conventional triaxial compression tests and one isotropic consolidation (compression) test, to establish the elastoplastic behaviour of the soil (Helwany 2007). Table 2 lists the parameters for the materials. A point at the center of manhole was selected to record displacement results because the maximum displacement

occurs at the center. Figure 11 shows the results when a double heavy load was applied. The results for each applied load shows the displacements at the same point, these compared with the results of the measurements taken at the cover of the manhole for the experimental tests, under the same series of loads.

Fig. 11. The displacement of the new manhole at a double heavy load shown in a 3D quarter symmetric FEA model.

The FE model output and the experiment model have a very close match regarding the displacement of the new manhole under live loads, as demonstrated in Figure 12.

Fig. 12. Comparison of the displacements from both the experimental work and the FE model for the new manhole, in soil, under live loads.

The same point was selected to show the displacement results for the traditional manhole, a sample of the results at a double heavy load are presented in Figure 13.

Fig. 13. The displacement of the traditional manhole at a double heavy load shown in a 3D quarter symmetric FEA model.

The comparison of the results from the FE model and the experiment model reveal a close match regarding displacement at low loads and between displacements for the traditional manhole under high live loads. The experimental measurements and FEA results gave a reliable assessment of the behaviour of the geometry of the manhole and estimations of the margins of error expected from the FEA. The experimental test and the FE model results for the traditional manhole are presented in Figure 14.

Fig. 14. Comparison of the displacement results from both experimental works and the FE model for the traditional manhole prototype in soil under live loads.

One of the important validation processes is the comparison of the FE model with lab experimental results to eliminate uncertainty and manage discrepancies in the model thus increasing confidence in the real application (Moser and Folkman 2008). Validation makes the designer more aware of the inevitable inaccuracies between a real case study and an FE model (Mar 2002). The two stages explained above, illustrate that all necessary steps to check and validate the accuracy of the FE model have been taken. All the boundary conditions, contact interactions, material properties and steps were identified correctly, meaning it was possible to upgrade the FE model to a real-life scale with confidence.

5.3 *The real FE model results*

Normally the dimensions of traditional manholes used in most sewer networks are 1 to 1.8 meters diameter, the depth ranging from 1 to approximately 7 meters. Real scale dimensions were selected for intermediate networks in the sewer system where new systems were expected to be located. The traditional manhole was 1.3 meters in diameter and 3.4 metre deep; the storm chamber of the new manhole 2.8 meters in diameter and 2.65 meters deep, the sanitary chamber having the same dimensions as the traditional manhole. The soil was of 8.5 meters radius and 15 meters deep to identify the maximum area affected by force (Brinkgreve 2013). The same soil properties as for the prototype model, were used for the real scale module. Non-reinforced concrete (Najafi and Sever 2015b), was used for the manhole material. The new manhole had 143345 nodes and 138100 elements element types (C3D6 & C3D8R). Figure 15 illustrates the setup of the new manhole in soil. Regarding the traditional manhole, the mesh used was finer to control for the instability found during experimental testing and to avoid aborting the test as a result of the substantial displacement that can occur. The number of nodes was 377705, 373240 elements, the element types the same as for the new manhole (C3D6 & C3D8R). Figure 16 illustrates the setup of the traditional manhole model in soil.

Fig. 15. Setup of the real scale of new manhole – soil model.

Fig. 16. Setup of the real scale of traditional manhole-soil model.

The data regarding the FE model were taken at the center point of the manhole base for both the new and traditional manhole. The maximum displacement at the base of the both manholes was identified. The new manhole is stable, even under high loading (loads 360 KN), the displacement of the soil below the manhole centerline being 8.16 mm, 3.55 mm under loading HS25 (90kN), 3.3 mm when the load was HS20 (70-80 kN) and approximately 3 mm when the load was HS15 (50-60kN). These results reflect high stability against very high loads, more than double the loads that normally occur. The displacements for the traditional manhole had less stability under high loads (loads 360 KN) because the area of the base is smaller than that of the new manhole. The displacement of soil below the manhole centerline was 11.8 mm at 360 kN, 3.4 mm when the load was HS25 (90kN), 3 mm when the load was HS20 (70-80 kN) and 2.7 mm when the load was HS15 (50-60kN). The traditional manhole has less displacement under medium loads and about the same displacement under heavy loads compared with the displacement of the new manhole under the same loads. It also experiences higher displacement under over-loads in comparison to the new manhole. The traditional manhole has less displacement under medium (HS15) loads compared to the new manhole, because of the increased weight of the new manhole which, this adding an extra load to the live load causing additional displacement. Figure 17 shows a comparison of the displacement of the soil below the new and traditional manholes.

Fig. 17. A comparison of the displacement for both manholes under different loads (FE model).

The results for displacement to both manhole covers and the soil surface for the new manhole, indicates that the new manhole has more impact on the surrounding soil as it was displaced between 1-2 mm, under medium and heavy loads (50 to 90 kN), affecting a 3-meter circle around the manhole. This displacement increased to between 2-3.5 mm under a double-heavy load. This displacement represents a summation of the soil displacement below the manhole and the deformation of the manhole material. The displacement increases from 8.16 mm to 9.95 mm under extreme loading, from 3.55 mm to 4 mm when the load was HS25 (90kN), from 3.3mm to 3.8 mm when the load was HS20 (70-80 kN) and from 3 mm to 3.48 mm when the load was HS15 (50-60 kN). These surface displacements need to be taken into consideration when designing road surfaces as the soil displacement below the manhole base effects connecting manhole pipes. This is critical in many cases of sewer collapse, the collapse happens at the connection joint between the pipes and the manhole because of relative displacement. There was less displacement with the new manhole model, both total surface and soil below the manhole. This increases the safety of sewer systems subject to very high loads. The stress results for the new manhole revealed that the maximum stress is on a slab positioned at the external wall of the storm chamber. The stress is decreased in the direction of the center of the manhole and increased slightly in the area close to the internal wall. The displacement occurring in the traditional manhole surface increased from 11.8 mm to 12.3 mm under high loads. This includes the displacement of the soil underneath manhole and the manhole structure deformation, from 3.4 mm to 3.6 mm when the load was HS25 (90kN), from 3 mm to 3.2 mm when the load was HS20 (70-80 kN) and from 2.7 mm to 2.85 mm when the load was HS15 (50-60kN). These results show that the traditional manhole has less displacement under medium loads and about the same displacement as the new manhole design under heavy loads. It has high displacement under over-loads which are close to failure at 13 mm. A smaller manhole has less impact on the surrounding surface soil, displacements between 1-2 mm across all loads. The stress in the surrounding soil generated by the traditional manhole structure was higher than the stress experienced by the new manhole. It was about three times higher, in comparison to the new manhole which has a larger surface area working to mitigate load stress effects. This reduction in stress is promising as it may allow the use of lightweight materials such as GRP, HDPE or PVC to build the whole, or part of, the

manhole structure, e.g. the inner chamber, while using concrete for the external chamber (the storm chamber). There is also the potential to decrease the thickness of the walls, or to minimise the amount of reinforced steel required.

5.4 *Investigation of manhole body structure*

The change in geometry of the manhole created a change in its structural behaviour. The non-reinforced traditional manhole has been previously tested by Sabouni and El Naggar (2011a) who used two manholes of 1200 mm and 1500 mm. They used 52 MPa as the cylinder compressive strength for the concrete of the base manhole, this a relatively high strength. Their results indicated that both manholes were able to withstand the applied loads, the maximum overall calculated strain approximately 75% in the 1200 mm manhole and 83% in 1500 mm manhole less than the base cracking strain. Sabouni and El Naggar (2011b) also generated a numerical model (FE) for both manholes. They found that the cracking moment (Mcr) of the manhole bases was 16.3 kN·m/m for the 1200 mm manhole and 62.4 kN·m/m for 1500 mm manhole, the average bending moment calculated at 4.8 kN·m for the 1200 mm manhole and 10.25 kN·m for the 1500 mm manhole. Further to this, Najafi and Sever (2015a) carried out testing and an FE study for a manhole of 1200 mm, reporting the maximum strain as 0.00019 and the maximum moment as 1 kN·m/m compared with a calculated cracking moment of 15.43 kN·m/m. They used non-reinforced concrete, which has a 40 MPa cylinder compressive strength. It should also be noted that they applied a low load (HS15), approximately 53 kN, to the manhole.

The same procedure and materials as used by Najafi and Sever (2015a) were used in this research. The applied load however was different as we applied conservative traffic loads to the manhole. Table 2 shows the properties of the concrete used for the manhole. ACI318 limits the strain in the concrete to 0.003. The cracking moment of the concrete is calculated using an ACI318 equation (3), 22.7 kN-m for the base of the traditional manhole and 34.1 kN-m for the new manhole. These limits were used to

compare the output of both structural manhole models. Table (3) illustrates the maximum strain on the manhole body and the percentage difference for the bending moment of the base manholes compared with the cracking moment.

According to ACI318 the cracking moment of the concrete is calculated as follows:

$$M_{cr} = \frac{f_{cr} I_g}{y_t} \quad \text{.....(Eq 2)}$$

For circular concrete slabs, it is

$$M_{cr} = \frac{f_{cr} b h^2}{6} \quad \text{.....(Eq 3)}$$

where Ig is the gross moment of inertia (m^4); b and h are the width and thickness of manhole base slab, and f_{cr} is the flexural cracking strength.

Figures 18a and b show the strain and location of the maximum bending moment in the base of the manhole for both the new manhole body and the traditional manhole body, under a double heavy load (180kN). The new manhole almost failed under double heavy loads, this the extreme case, while the traditional manhole was able to withstand this extent of loading. Double heavy loads are used in this study to test the maximum structural capacity of the manhole. The manhole body structure will be studied in detail using reinforced concrete and light-weight materials such as GRP or HDPL in a subsequent study. We will also investigate if the provision of a flexible joint between the sanitary wall chamber and the base of storm chamber can improve the structural performance of the manhole. The structure of the new manhole body can effected by the degree of compaction of the soil underneath the two chambers of the manhole. Any difference in soil stiffness below these chambers can led to differential settlement which generates more stress in the body of the manhole depending on the location of the applied load. Therefore, reinforced concrete is required for the new manhole design when it is not being laid in a narrow street and can be exposed to double heavy loads.

Fig. 18 a. The strains and location of maximum bending moment in the base of the new manhole body under a double heavy load (180kN).

Fig. 18 b. The strains and location of maximum bending moment in the base of the traditional manhole body under a double heavy load (180kN).

6. Conclusions

The technological development of inspection and maintenance equipment for sewer systems, in combination with the availability of new materials for pipe and manhole manufacture, has allowed improvements to be made to traditional manholes. Environmental regulations in many developed and developing countries, require separate sewer systems to be built as combined sewer systems are no longer acceptable. As a response, this research has presented a new design for manholes, siting the two traditional separate sewer system manholes together in one manhole structure, improving on the installation method of separate sewer systems in narrow streets. It has two separate chambers; an external chamber used to carry storm flow and an inner chamber used for sewage flow. Because of the design, it is bigger and heavier in comparison to the traditional manhole. Structural performance testing was carried out using 3D finite element analysis and compared to the performance of traditional manholes. The results revealed that:

- The weight of the new manhole added a dead load to the loads applied, this affecting the behaviour of the manhole. The displacement was higher than that for a traditional manhole under a small live load.
- Under heavy loads, both the new and traditional manhole exhibit the same behaviour (settlement) and both operate within standard limitations.
- The new manhole has very good stability under extremely high loads; the traditional manhole experienced more settlement under the same load.
- The new manhole was stable and had less displacement under a double heavy load. However, the bending moment was close to the cracking moment at the base of the storm chamber under a double heavy load; reinforcement was recommended for the slab (cover) and the base of the manhole. This will be examined in the next stage of the current research.
- The levels of soil stress in the new manhole were dramatically reduced, in comparison to soil stress in the traditional manhole structure, under identical loads.

The structural improvements generated by the mathematical model (successfully calibrated by the experimental work), allow the safe use of this new manhole in narrow streets, prevalent in the UK and

EU, which up to now have constituted a real challenge when constructing traditional separate sewer systems. The displacement of the new manhole is higher than the displacement of the traditional manhole, under low loads, because of the weight of the new manhole. This effect is expected to disperse through the construction stage under good compaction processes. The new manhole shows high stability and resistance against high live loads. The stress created by live loads on the new manhole was significantly lower than that for traditional manholes. This implies that a review can be made of the thickness and reinforcement required for the walls of the manhole, including the potential to use lighter materials such as GRP, HDPE and PVC in the manufacture of new structures.

Acknowledgements

The first authors would like to express their sincere thanks to the Al Ghalowa Company for their support. Thanks are also extended to LJMU technical staff for providing the necessary support to carry out the experimental testing.

References:

Abbas, A., Ruddock, F., Alkhaddar, R., Rothwell, G., and Andoh, R. 2017. Pipeline–Soil Interaction Simulation under Live Loads Using Elastoplastic Finite Element Models with Laboratory Validation, California, USA ASCE.

Abolmaali, A., and Kararam, A. 2010. Nonlinear Finite-Element-Based Investigation of the Effect of Bedding Thickness on Buried Concrete Pipe. Journal of Transportation Engineering **136**(9): 793-799.

ACPA, A.C.P.A. 2008. Design data 20: Circular precast concrete manhole. American Concrete Pipe Association, Virginia, USA.

Ahn, N., Park, D.K., Lee, J., and Lee, M.K. 2009. Structural test of precast polymer concrete. Journal of Applied Polymer Science **114**(3): 1370-1376.

Al-Saleem, H.I., and Langdon, W. 2016. Precast Concrete Manholes - A review and Upgrade of Current Practice. *In* WATER NEW ZEALAND 2016 STORMWATER CONFERENCE, NEW ZEALAND.

ASTM-C890. 2006. Standard Practice for Minimum Structural Design Loading for Monolithic or Sectional Precast Concrete Water and Wastewater Structures. American Section of the International Association for Testing Materials, United States.

Bandler, A. 2007. The Structural Capacity of Repaired Manholes, Department of Civil Engineering, Queen's University, Kingston, Canada.

Bettez, J., Townsend, R.D., and Comeau, A. 2001. Scale model testing and calibration of City of Ottawa sewer weirs. Canadian Journal of Civil Engineering **28**(4): 627-639.

Bizier, P. 2007. Gravity Sanitary Sewer Design and Construction. American Society of Civil Engineers, USA

Brinkgreve, R.B.J. 2013. Validating Numerical Modelling in Geotechnical Engineering. NAFEMS.

Brown, S.F., and Brown, C.J. 2000. The structural characteristics of manhole installations in pavements.

BS. 2010. BS 9295:2010 - Guide to the structural design of buried pipelines. BSI, UK.

BSEN476. 2011. Generla requirements for components used in drains and sewers. BSI British Standards, UK. p. 25.

BSEN752:2008. 2013. Drain and sewer systems outside buildings. British Standards, UK.

CPAA, C.P.A.o.A. 2016. Loads on Circular Precast Concrete Manholes and Access Chambers. *In* GUIDANCE NOTE (NZ), Australia. p. 8.

524 DEFRA. 2011. National Build Standards Design and Construction of new gravity foul sewers and
525 lateral drains. *In* Water Industry Act 1991 Section 106B, Flood and Water Management Act 2010
526 Section 42. Department for Environment Food and Rural Affairs, UK. p. 36.

527 EPA, U.S.E.P.A. 2007. Innovation and Research for Water Infrastructure for the 21st Century, USA.

528 Helwany, S. 2007. Applied Soil Mechanics with ABAQUS Applications. John Wiley & Sons, Inc.,
529 Hoboken, NJ, USA.

530 Hughes, J.B. 2009. Manhole Inspection and Rehabilitation. American Society of Civil Engineers
531 ASCE, Reston, Va.

532 IKT, I.f.U.I. 2012. Rehabilitation of Wastewater Manholes: Large Scale Tests ans in-Situ Studies
533 Institute for Underground Infrastructure, Germany

534 Lees, A. 2012. Obtaining Parameters for Geotechnical Analysis. NAFEMS.

535 Mar, A. 2002. How To Undertake Finite Element Based Geotechnical Analysis. NAFEMS.

536 Moser, A.P., and Folkman, S. 2008. Buried Pipe Design McGraw-Hill.

537 Najafi, M., and Sever, V.F. 2015a. Structural Capabilities of No-Dig Manhole Reha. Water
538 Environment Research Foundation, USA

539 Najafi, M., and Sever, V.F. 2015b. Structural Capabilities of No-Dig Manhole Rehabilitation. Water
540 Environment Research Foundation.

541 Petroff, L.J. 1994. Design methodology for high density polyethylene manholes. *In* Buried Plastic
542 Pipe Technology. *Edited by* D. Eckstein. ASTM STP 1222. pp. 52–65.

543 Sabouni, R., and El Naggar, M.H. 2011a. Circular precast concrete manholes: experimental
544 investigation. Canadian Journal of Civil Engineering **38**(3): 319-330.

545 Sabouni, R., and El Naggar, M.H. 2011b. Circular precast concrete manholes: numerical modeling.
546 Canadian Journal of Civil Engineering **38**(8): 909-920.

547 Saricimen, H., Shameem, M., Barry, M.S., Ibrahim, M., and Abbasi, T.A. 2003. Durability of
548 proprietary cementitious materials for use in wastewater transport systems. Cement and Concrete
549 Composites **25**: 421-427.

550 Torben Pichler, T.P., Thorben Hamann, Sascha Henke, Gang Qiu. 2012. High-Performance Abaqus
551 Simulations in Soil Mechanics Reloaded – Chances and Frontiers, USA, May 15-17, Dassault
552 Systèmes

553 Willi, G. 1998. Schacht für Kontroll-, Wartungs- oder Reparaturarbeiten *Edited by* E.P. Office,
554 Germany. p. 2.

555 Würmseher, H. 2014. Abwasserschacht (Manhole) *Edited by* D.P.-u. Markenamt, Germany p. 7.

Table 1: Vehicle load designations

Designation	Load, max	Uses
ASTM HS25	(89 200 N) per wheel	heavy traffic
ASTM HS20	(71 200 N) per wheel	heavy traffic
ASTM HS15	(53 400 N) per wheel	medium traffic
ASTM H10	(35 600 N) per wheel	light traffic
Extreme heavy load	185 kN 207 kN	One wheel from 4th axle (heaviest wheel load) with load factors 2.1 and 2.4 (Sabouni and El Naggar 2011b)
Loading according to BS 5400□2:1978) citied in BS 9295:2010	2 × 112.5 kN	**Main roads** 112.5 kN wheel loads including an impact factor of 1.3
	2 × 105 kN	**Light trafficked roads** 105 kN wheel loads including an impact factor of 1.5
	2 × 60 kN	**Fields** 60 kN wheel loads, including an impact factor of 2.0

Table 2: Model parameters

Items	Parameters	Value		
	Density	1685 kg/m^3		
	E	16.943 MPa		
	υ	0.295		
Soil	**Drucker –Prager**			
	β	50		
	K	0.8		
	ψ	15		
	Density	7850 kg/m^3		
Steel	E	210GPa		
	υ	0.3		
	Density	1855 kg/m^3		
	E	100MPa		
Bedding	ϕ	35		
	C	0		
	υ	0.4		
	Density	2200 kg/m^3		
	E	29,992 MPa		
	υ	0.2		
	Plasticity			
	Dilation Angle	38		
	Eccentricity	0.1		
	f_{b0}/f_{c0}	1.16		
Concrete	K	0.667		
	Viscosity Parameter	10^{-7}		
	Compressive Behaviour			
	Yield stress	27,000 kPa	39,990 kPa	
	Inelastic Strain	0	0.01	
	Tensile Behaviour			
	Yield stress	5000 kPa	2200 kPa	50 kPa
	Cracking strain	0	0.006	0.015

Table 3. Percentage difference for the bending moment of the manhole bases, the cracking moment and the maximum strain on the body of the manhole.

	New Manhole design			**Traditional manhole design**		
Load categories	Bending moment	% Diff from the M_{cr}	Max Strain	Bending moment	% Diff from the M_{cr}	Max Strain
HS15	11.9	65%	$4.29x10^{-5}$	4.27	81%	$3.6x10^{-5}$
HS20	13.73	60%	$4.89x10^{-5}$	4.87	78%	$4.1x10^{-5}$
HS25	15.38	55%	$5.5x10^{-5}$	5.46	75%	$4.5x10^{-5}$
Double heavy load	30.23 – 33.54	11% -1.7%	$1x10^{-4}$– $1.2x10^{-4}$	10.68 – 11.815	53% - 48%	$8.9x10^{-5}$– $9.8x10^{-5}$

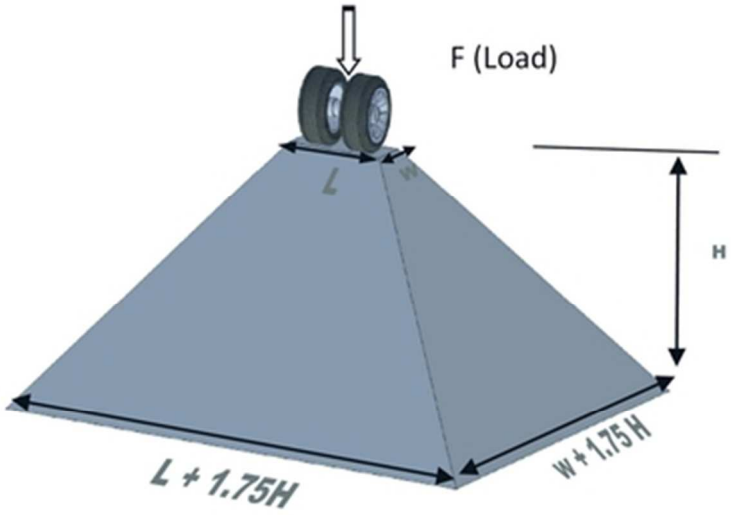

Figure 1. Pyramid method for the distribution of a live load

Fig. 1. Pyramid method for the distribution of a live load "Reproduced, with permission from [ASTM C890-13] ASTM International"

75x54mm (150 x 150 DPI)

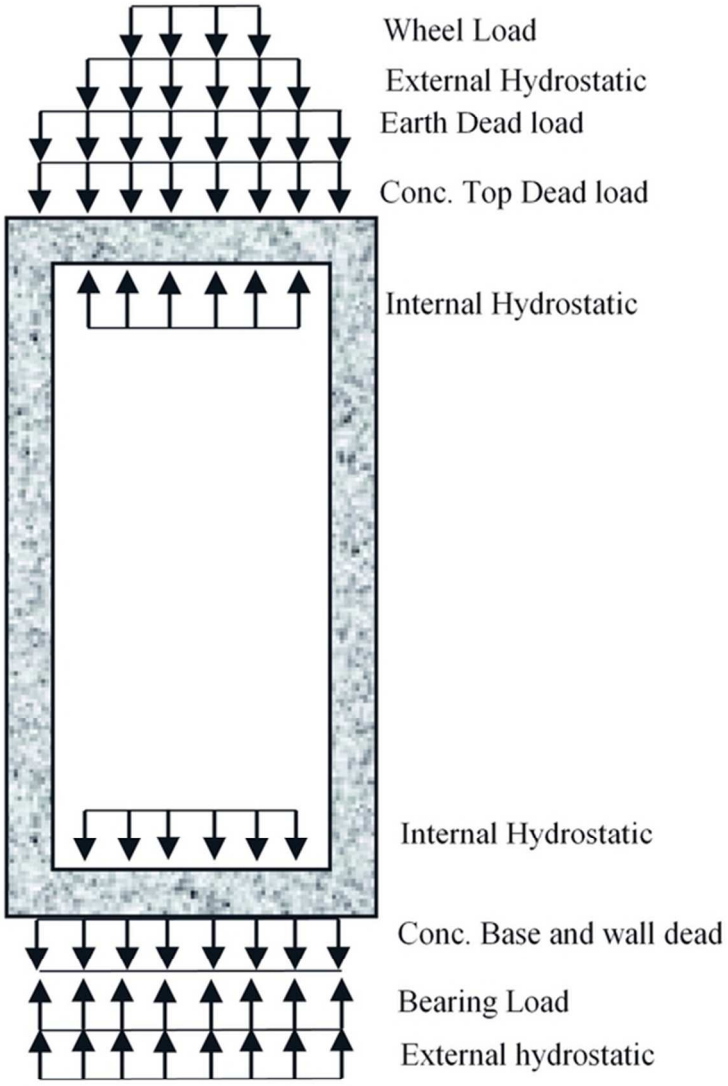

Figure 2. Cumulative vertical loads

Fig. 2. cumulative vertical loads "Reproduced, with permission from [ASTM C890-13] ASTM International"

107x148mm (150 x 150 DPI)

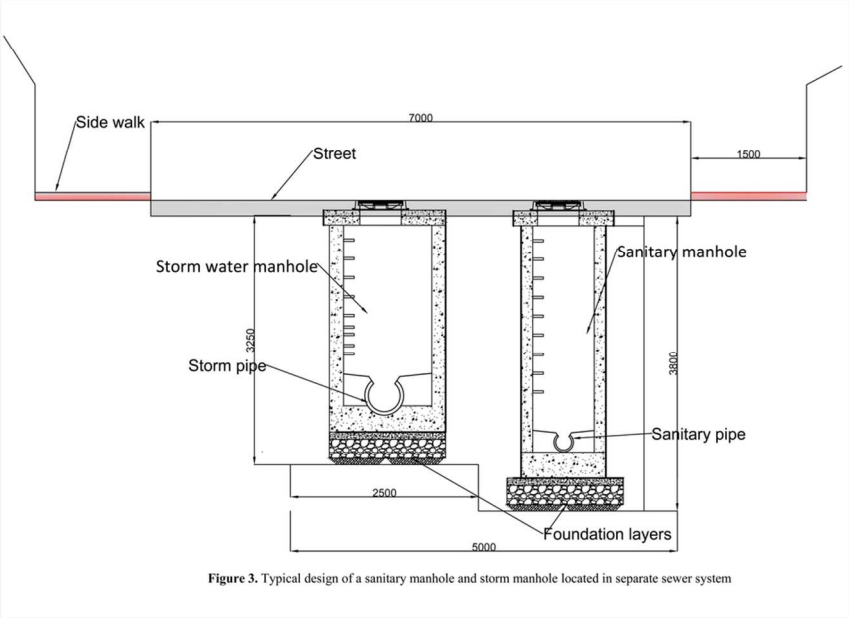

Figure 3. Typical design of a sanitary manhole and storm manhole located in separate sewer system

Fig. 3. Typical design of a sanitary manhole and storm manhole located in a separate sewer system
‼ ┼ ‼ ┼ ‼ ┼

209x148mm (150 x 150 DPI)

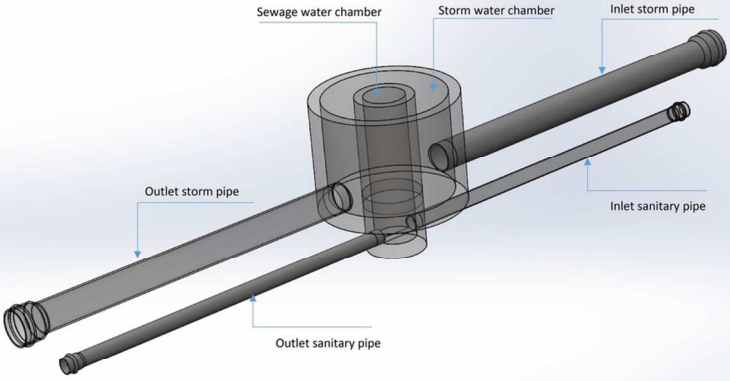

Figure 4. Innovative design of manhole for separate sewer system.

Fig 4. Innovative design of a manhole for separate sewer systems.

209x148mm (150 x 150 DPI)

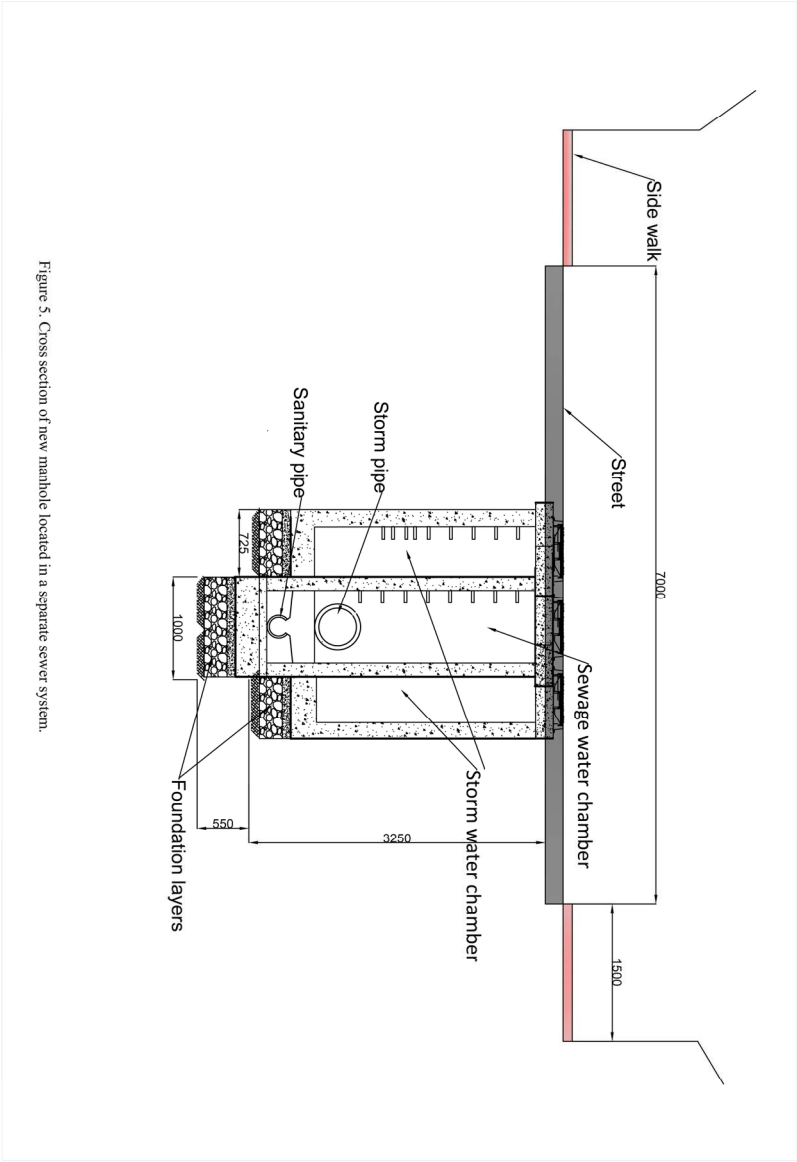

Figure 5. Cross section of new manhole located in a separate sewer system.

Fig. 5. Cross section of new manhole located in a separate sewer system.

297x420mm (150 x 150 DPI)

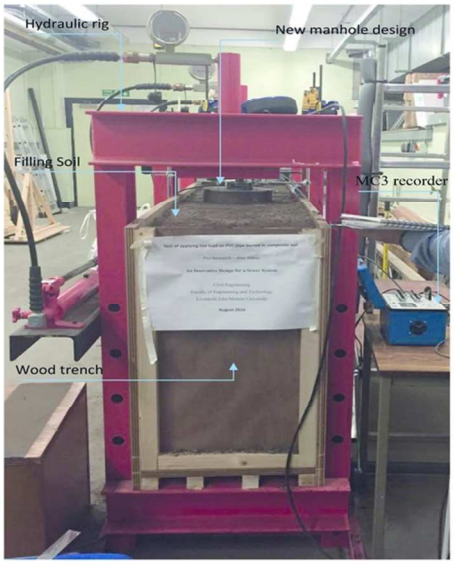

Fig. 6 a. Setup of the trench in the rig and location of measurement instruments on the new manhole surface at three points on the edge.

Fig. 6 b. Setup of the trench in the rig and location of measurement instruments on the new manhole surface at three points on the edge.

Fig. 6 a and b. Setup of the trench in the rig and location of measurement instruments on the new manhole surface at three points on the edge.

179x110mm (150 x 150 DPI)

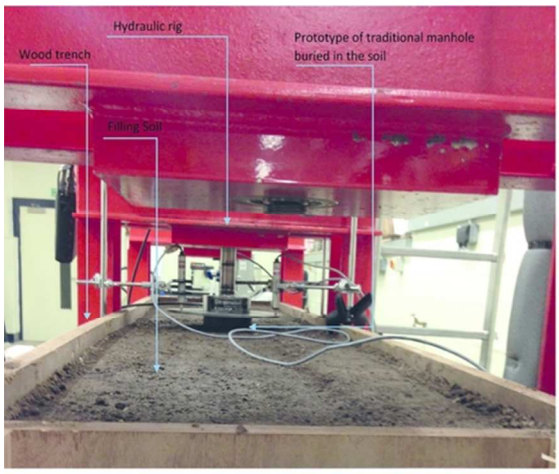

Fig. 7 a. Setup of the trench in the rig and location of measurement instruments on the traditional manhole surface at three points on the edge.

Fig. 7 b. Setup of the trench in the rig and location of measurement instruments on the traditional manhole surface at three points on the edge.

Fig. 7 a and b. Setup of the trench in the rig and location of measurement instruments on the traditional manhole surface at three points on the edge.

138x72mm (150 x 150 DPI)

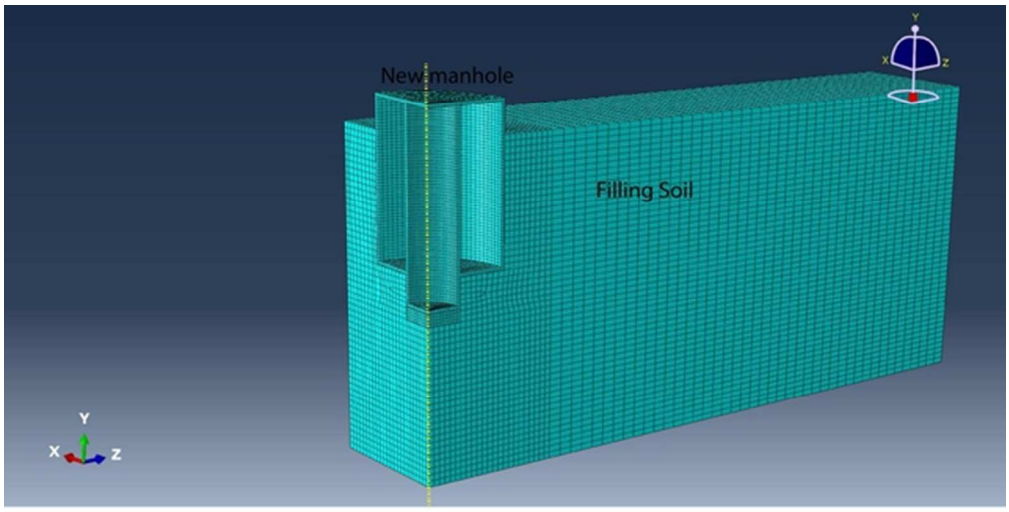

Figure 8. The symmetrical quarter of the new manhole FE mesh model represented the fully 3 D Manhole

Fig. 8. The symmetrical quarter of the new manhole FE mesh model representing the full 3D manhole

108x63mm (150 x 150 DPI)

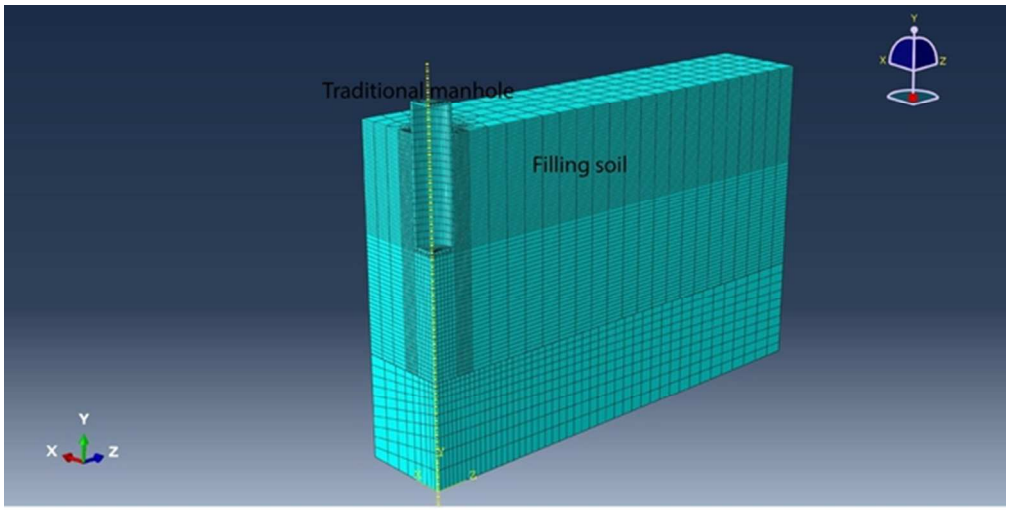

Figure 9. The symmetrical quarter of the traditional manhole FE mesh model represented the fully 3 D Manhole

Fig. 9. The symmetrical quarter of the traditional manhole FE mesh model representing the full 3D manhole

107x63mm (150 x 150 DPI)

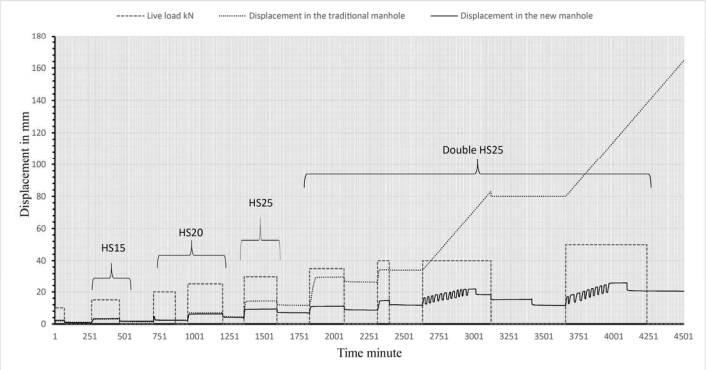

Fig. 10. Comparison between the new and traditional manholes under the same conditions and live loads.

Fig. 10. Comparison between the new and traditional manholes under the same conditions and live loads.

297x420mm (150 x 150 DPI)

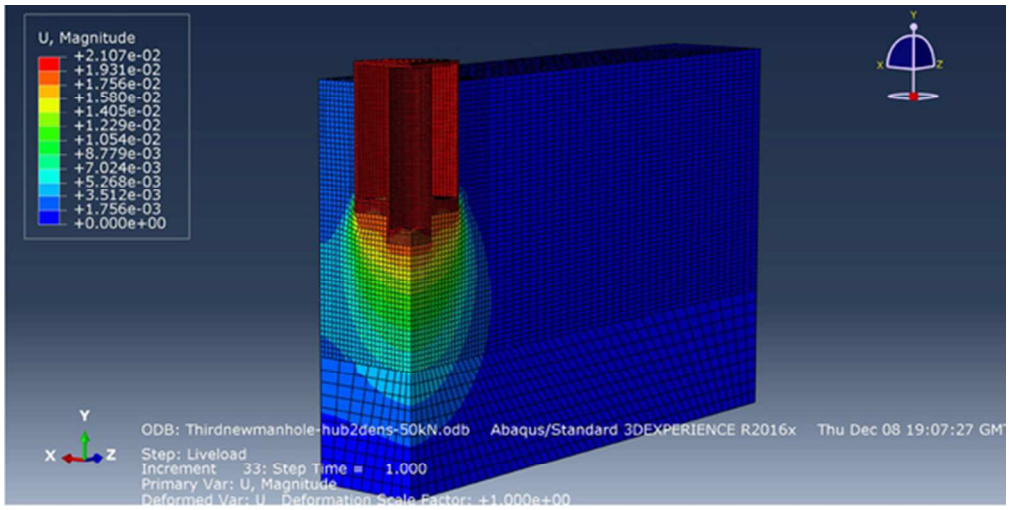

Fig. 11. The displacement of the new manhole at a double heavy load shown in a 3D quarter symmetric FEA model.

Fig. 11. The displacement of the new manhole at a double heavy load shown in a 3D quarter symmetric FEA model.

101x55mm (150 x 150 DPI)

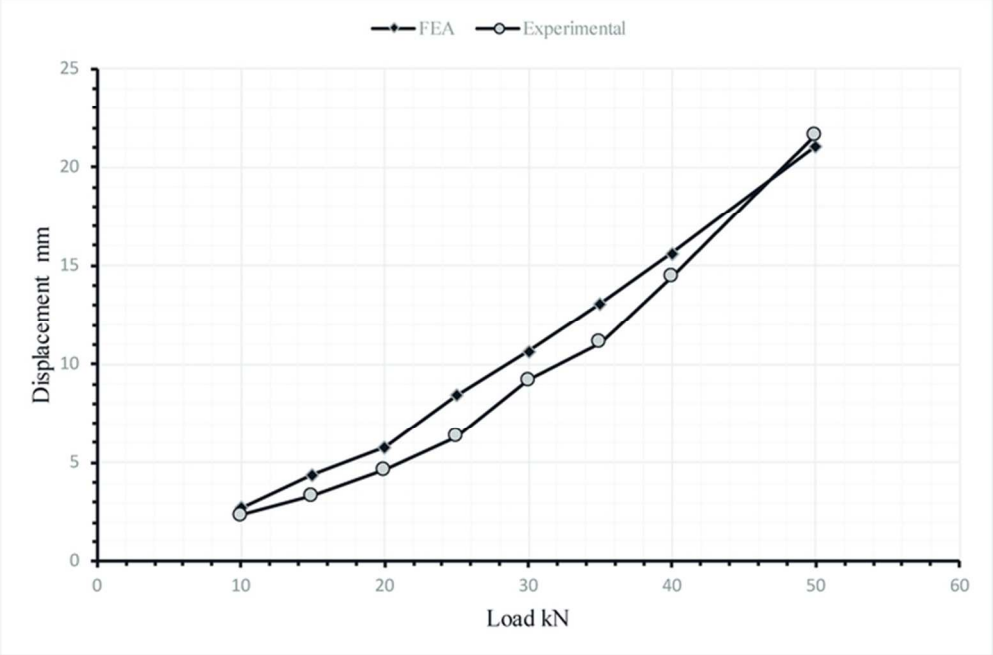

Fig. 12. Comparison of the displacements from both the experimental work and the FE model for the new manhole, in soil, under live loads.

Fig 12. Comparison of the displacements from both the experimental work and the FE model for the new manhole, in soil, under live loads.

128x96mm (150 x 150 DPI)

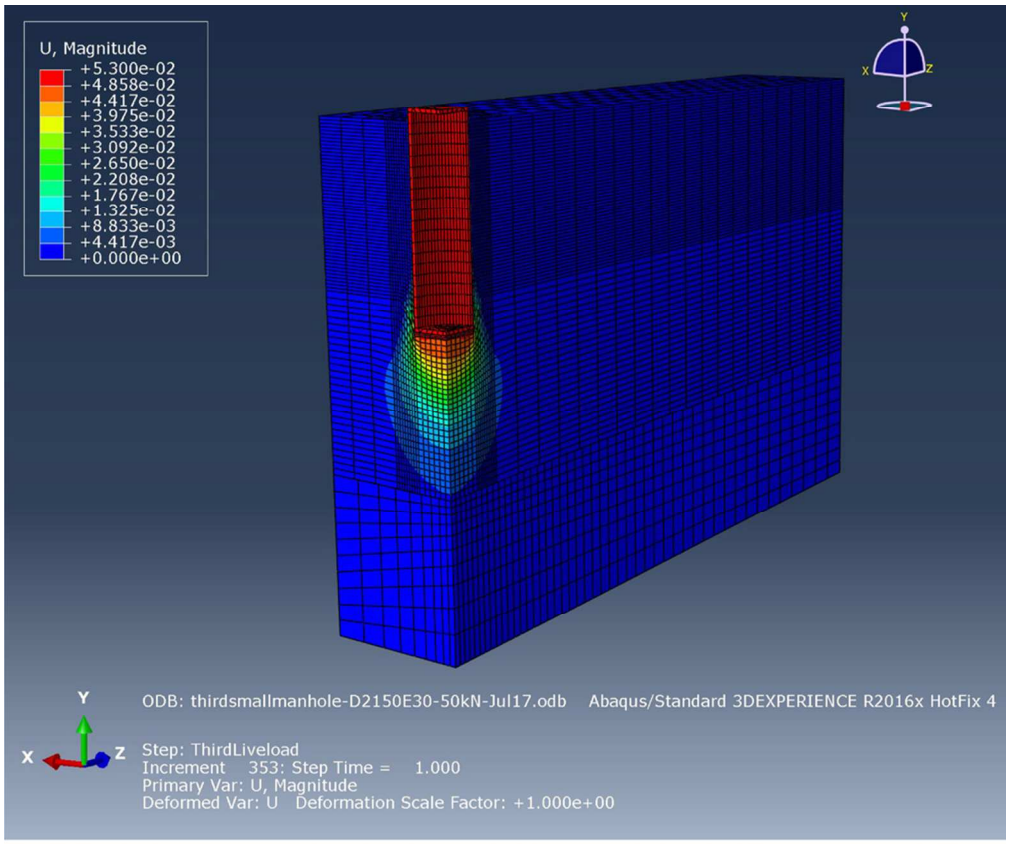

Fig. 13. The displacement of the traditional manhole at a double heavy load shown in a 3D quarter symmetric FEA model.

Fig. 13. The displacement of the traditional manhole at a double heavy load shown in a 3D quarter symmetric FEA model.

167x152mm (150 x 150 DPI)

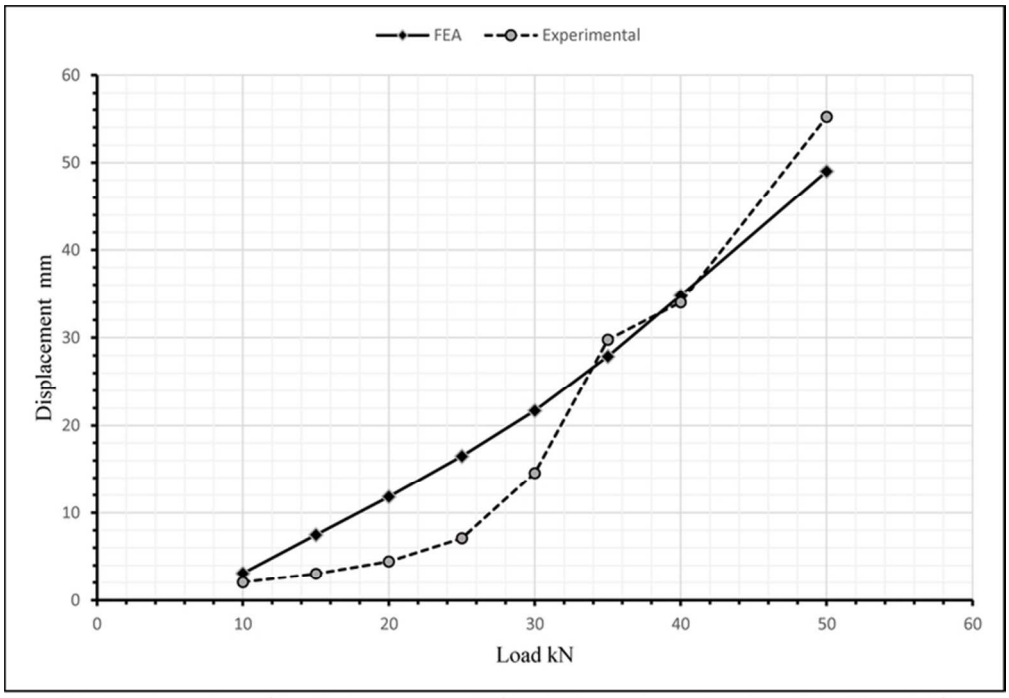

Fig. 14. Comparison of the displacement results from both experimental works and the FE model for the traditional manhole prototype in soil under live loads.

Fig. 14. Comparison of the displacement results from both experimental works and the FE model for the traditional manhole prototype in soil under live loads.

132x100mm (150 x 150 DPI)

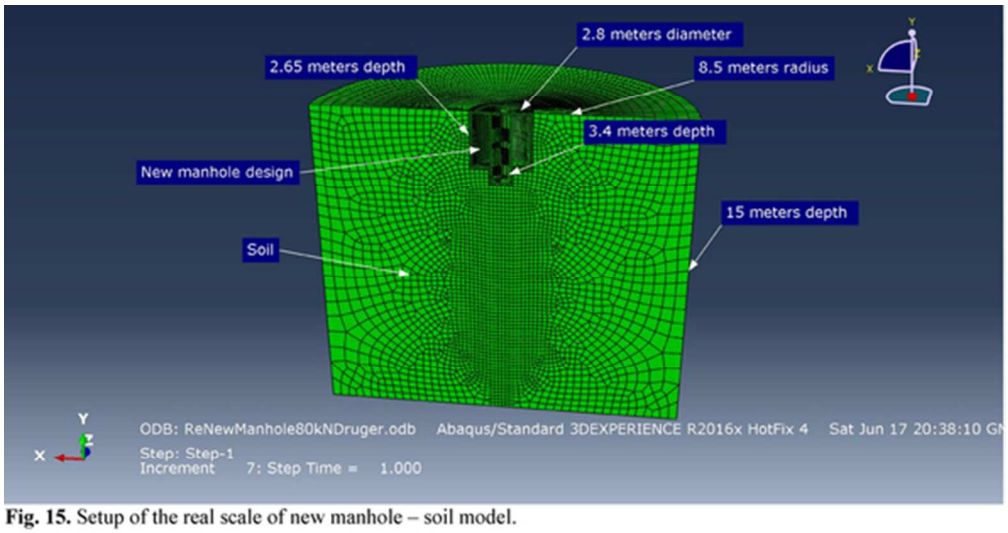

Fig. 15. Setup of the real scale of new manhole – soil model.

Fig 15. Setup of the real scale of new manhole – soil model.

100x54mm (150 x 150 DPI)

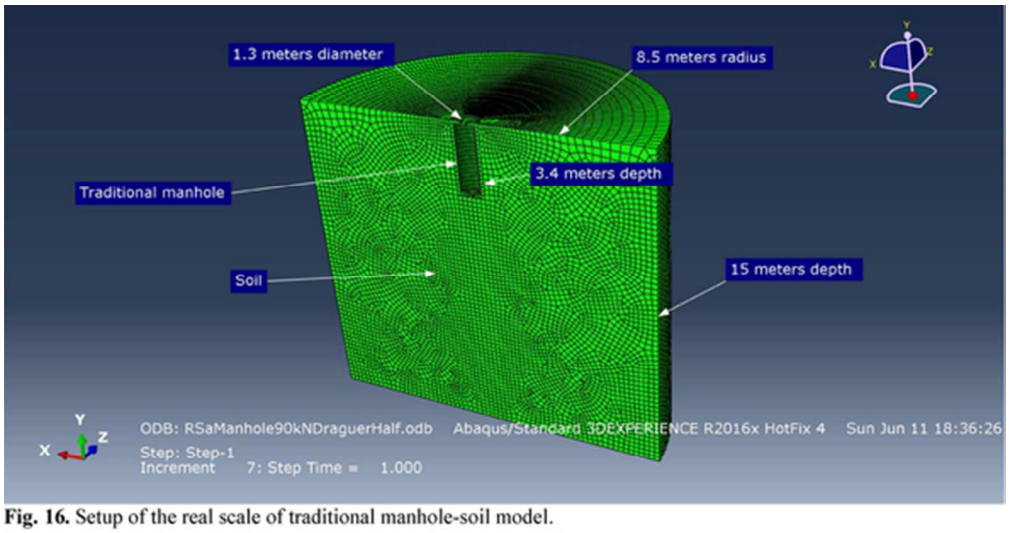

Fig. 16. Setup of the real scale of traditional manhole-soil model.

Fig. 16. Setup of the real scale of traditional manhole-soil model.

99x54mm (150 x 150 DPI)

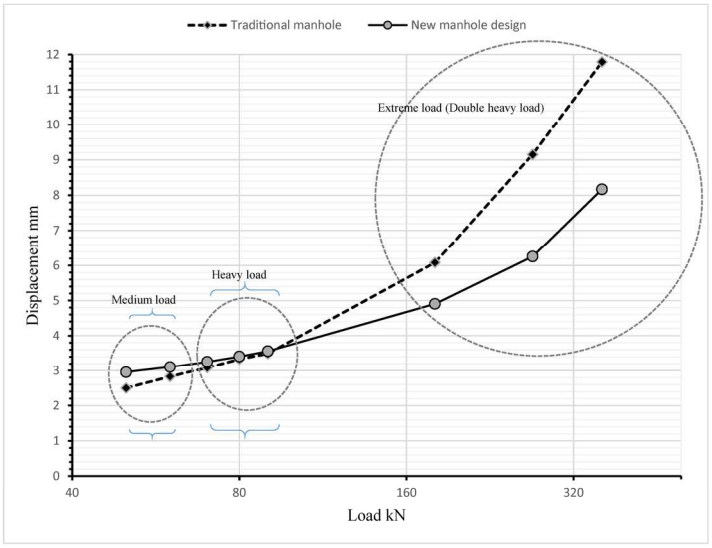

Fig. 17. A comparison of the displacement for both manholes under different loads (FE model).

Fig. 17. A comparison of the displacement for both manholes under different loads (FE model).

297x420mm (150 x 150 DPI)

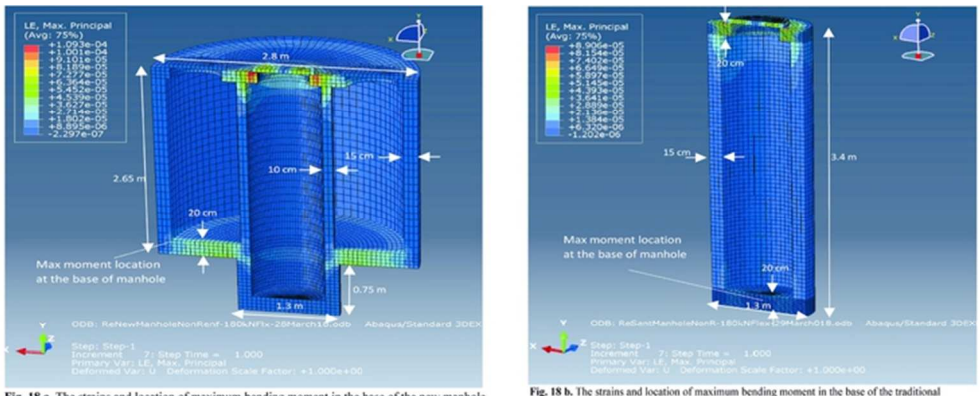

Fig. 18 a. The strains and location of maximum bending moment in the base of the new manhole body under a double heavy load (180kN).

Fig. 18 b. The strains and location of maximum bending moment in the base of the traditional manhole body under a double heavy load (180kN).

Fig. 18 a. The strains and location of maximum bending moment in the base of the new manhole body under a double heavy load (180kN).

Fig. 18 b. The strains and location of maximum bending moment in the base of the traditional manhole body under a double heavy load (180kN).

126x53mm (150 x 150 DPI)